

Invited Review

CLOUDY 90: Numerical Simulation of Plasmas and Their Spectra

G. J. FERLAND,¹ K. T. KORISTA,^{1,2} D. A. VERNER,¹ J. W. FERGUSON,^{1,3} J. B. KINGDON,^{1,4} AND E. M. VERNER¹

Received 1998 January 19; accepted 1998 March 3

ABSTRACT. CLOUDY is a large-scale spectral synthesis code designed to simulate fully physical conditions within an astronomical plasma and then predict the emitted spectrum. Here we describe version 90 (C90) of the code, paying particular attention to changes in the atomic database and numerical methods that have affected predictions since the last publicly available version, C84. The computational methods and uncertainties are outlined together with the direction future development will take. The code is freely available and is widely used in the analysis and interpretation of emission-line spectra. Web access to the Fortran source for CLOUDY, its documentation Hazy, and an independent electronic form of the atomic database is also described.

1. INTRODUCTION

The physical conditions within any low-density astronomical plasma are governed by a host of microphysical processes. Together, these processes set the ionization distribution, level populations of excited states, and the electron temperature. The observed spectrum is the result of the transport of radiation through the depth-dependent physical conditions. No analytical solutions are possible because of the intricacies, and large-scale numerical simulations must be performed instead. Such simulations are a powerful complement to new generations of astronomical instrumentation—astronomical spectra can be interpreted on a quantitative basis. The majority of the quantitative information we have about the cosmos is the result of such spectroscopy.

Spectral synthesis codes are at the forefront of modern computational astrophysics. Ferland et al. (1995) give a summary of a number of plasma and shock codes. Most have similar overall structures and approaches. An optically thick slab of gas is divided into a large number of zones, chosen so that conditions are fairly constant across each. The level of ionization is determined by balancing all ionization and recombination processes. Ionization processes include photo, Auger, and collisional ionization and charge transfer. Recombination processes include radiative, low-temperature dielectronic, high-temperature dielectronic, three-body recombination, and charge transfer. The free electrons are assumed to have a predominantly Maxwellian velocity distribution with a kinetic temperature determined by the balance between heating (photoelectric,

mechanical, cosmic-ray, etc.) and cooling (predominantly inelastic collisions between electrons and other particles) processes. The associated line and continuum radiative transfer must be solved simultaneously. Papers that set the standards of the field include Hjellming (1966), Williams (1967), Rubin (1968), Harrington (1969), Davidson (1972), MacAlpine (1971), and Shields (1974). More recent studies include Binette et al. (1993), Petitjean, Boisson, & Pequignot (1990), Kallman & McCray (1982), Sutherland & Dopita (1993), Stasinska & Leitherer (1996), and Gruenwald, Viegas, & Brogiere (1997). Davidson & Netzer (1979), Osterbrock (1989), and Netzer (1990) give excellent reviews.

This paper is a progress report on the development of CLOUDY, a code designed to perform such simulations. CLOUDY was born at the Institute of Astronomy, Cambridge, in August of 1978. Since then it has gone through some 90 major revisions and has grown to include well over 10^5 lines of FORTRAN. The major long-term goal has been to simulate conditions in the broad-line regions (BLRs) of quasars, in order to calibrate them as probes of the universe at redshifts between 1 and 5. Galactic nebulae are also a major emphasis since they both serve as plasma laboratories and affect nucleosynthesis as the endpoints of stellar evolution. CLOUDY is used extensively by us here in Lexington, and it is available on the World Wide Web. Others across the astronomical community use it to publish more than 70 papers per year on topics ranging from the intergalactic medium and interstellar medium to nova envelopes and accretion disks. A list of publications that cited use of the code is available on the Web.

The goals of this paper are to outline the advances in the current version over 84.12a, the last publicly released version. Although the final version of C84 was released in mid-1993, its design and atomic database were fixed by early 1992. The growth in both the power of high-end workstations and in the breadth and quality of the underlying database have been explosive since that time. Version 90 was first released in June

¹ Physics Department, University of Kentucky, 177 CP Building, Lexington, KY 40506.

² Current address: Western Michigan University, Department of Physics, Kalamazoo, MI 49008.

³ Current address: Physics Department, Box 32, Wichita State University, Wichita, KS 67260-0032.

⁴ Current address: Space Telescope Science Institute, 3700 San Martin Drive, Baltimore, MD 21218.

of 1996 and has gone through four revisions as of this writing. We describe differences between the two versions, including why they may not agree, and outline the remaining uncertainties. We also describe Web access to CLOUDY and its documentation Hazy (§ 7).

Spectral synthesis codes are possible only because of the work of many atomic physicists, since the conditions in a non-equilibrium plasma are the result of a host of microphysical processes. We have made a major effort to consolidate this atomic database into convenient numerical packages. These are independently available on Dima Verner's Atomic Data for Astrophysics (ADfA) Web page (see § 7). The ADfA forms a tool kit for others to use to perform similar calculations. In the following we will identify the ADfA routines used to provide rates for specific physical processes.

2. HYDROGEN

The hydrogen atom must be treated completely, since its photoionization is the primary heating mechanism in nebulae and its opacity strongly affects a cloud's structure.

2.1. The Atom's Structure

Versions before CLOUDY 84 (C84) used the very compact H atom described by Cota (1987). This model atom had $1s$, $2s$, and $2p$ levels represented, as well as levels 3–6 assumed to be completely l -mixed. These core levels were supplemented by three higher pseudolevels designed to simulate the actual atom's levels n from 7 through 1000 as bands. This allowed the atom to go to LTE in a continuous manner at high densities. They were necessary since a finite atom, especially one with a dozen or fewer levels, would not have high levels in equilibrium with the continuum. These pseudolevels had large statistical weights and could contain a substantial fraction of the atom's population at high densities and temperatures.

The Cota (1987) model atom reproduced emission from the hydrogen atom in the high-density (well l -mixed) limit, went to LTE when irradiated by a blackbody or when the gas density was high, and worked very well in the nebular, or low-density, limit. However, tests have shown that this approach did not give a good representation of the physics of induced transitions within high levels for intense nonthermal continua. It also did not reproduce the expected theoretical intensities of many IR lines at low or intermediate densities because the well l -mixed approximation is not valid.

The current version uses the approach described by Ferguson & Ferland (1997; hereafter FF). It retains the essential physics of the real atom, with all levels having energies and statistical weights characteristic of true levels within the actual atom, while not resolving the l -states other than $2s$ and $2p$. In nature, at low densities, only the np states can directly decay to ground and so can be strongly depleted by emission of Lyman line radiation. The populations of the remaining l levels are set by the capture cascade problem (Seaton 1959), and these tend to

bunch up at the highest possible l state, which has only one decay route ($l \Rightarrow l - 1$). This is the low-density limit. At high densities, the levels are well l -mixed and transition probabilities go over to those listed by Wiese, Smith, & Glennon (1966, pp. 2–6). The result is that the populations of l states within an n level have strong density dependencies, and the total transition probabilities coming from a level do as well. As an example, the $\text{Pa}\alpha$ and $\text{H}\beta$ lines have a common upper level, but their intensity ratio changes by 50% between the low- and high-density limits (Storey & Hummer 1995; hereafter SH). The H atom in C84 and before reproduced only the high-density limit.

SH give the definitive results for emission from 1000 n -level atoms over a wide range of conditions, in a convenient electronic form. Their results are given for an extensive range of densities and go over to both low- and high-density limits. We have used these as a template in developing our atom. We were able to reproduce their results by allowing the branching ratios for the lowest 15 levels to depend on density and temperature, with the limiting branching ratios chosen to reproduce the asymptotic SH results.

In practice a compact atom is desired for computational speed, but a large atom is needed if the upper levels are to go to LTE in a continuous manner. In our implementation, the number of levels can be set at run time. We have experimented with atoms of various sizes up to 50 levels, but we find that 15 levels are generally sufficient for accurately describing emission from low-lying levels under nebular conditions. This is the default. More levels are needed for accurate representations of the higher states producing mid- to far-infrared emission.

2.2. Total Recombination Rates

Verner & Ferland (1996) computed total radiative recombination coefficients for hydrogenic atoms and ions. These are used to "top off" the model atom's total radiative recombination coefficient. The total recombination coefficient of our finite number of levels is a good fraction of the total. The remaining recombination coefficient must be added to the atom if the ionization balance is to be correct and must be distributed over a range of levels. This is because placing it into a single level would lead to an artificial overpopulation of that level and strong maser effects in transitions between it and lower levels. The highest five levels are assigned the remaining recombination coefficient, so that the sum is correct. This choice was made to obtain the best agreement with the SH results. The user can easily change both the number of levels and the way the model atom is topped off.

2.3. Collision Rates

We use Voronov (1997) for collisional ionization from the ground state and Vriens & Smeets (1980) for collisional ionization from excited levels.

Collisional excitation rate coefficients for the lower three levels of hydrogen are now taken from Callaway (1994). We

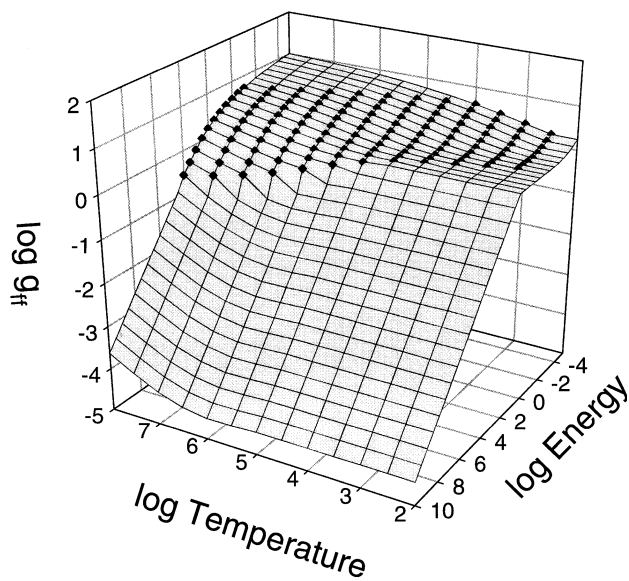


FIG. 1.—Logarithmic thermally averaged free-free Gaunt factors as a function of gas temperature and photon energy used in CLOUDY. The points shown are from Hummer (1988), while the rest are asymptotic limits from Rybicki & Lightman (1979).

take rates for collisions between $2s$ and $2p$ from Osterbrock (1989); this includes the important effects of proton collisions. For higher levels there is no definitive data source (see Chang, Avrett, & Loeser 1991), and we use the Vriens & Smeets (1980) semiempirical formulae since they extend over a wide range of temperature.

SH used collisional ionization rates from Burgess & Percival (1968) and Summers (1974) and collisional excitation rates from Percival & Richards (1978) for excited states and Aggarwal (1983a) and Hata, Morgan, & McDowell (1980) for $1s$, $2s$, $2p$, and 3 . These rates differ from the data set we use, and this is the largest source of uncertainty for the hydrogen atom. The Percival & Richards data set was intended only for use at relatively high energies. They quote the range of validity for collisions from lower level n as $1.6 \times 10^5 Z^2/n^2 \text{ K} < T \ll 3 \times 10^9 \text{ K}$. This data source is not expected to be reliable for the full range of levels and temperatures used by SH.

2.4. Overall Accuracy

The compact atom predicts $H\beta$ emissivities and relative intensities of lower lying lines, in excellent agreement with SH for temperatures greater than 10^3 K . For densities less than 10^{12} cm^{-3} , the differences are less than 5%, increasing to 30% for densities approaching 10^{14} cm^{-3} . For nebular temperatures (5000–20,000 K) and the full range of densities (10^2 – 10^{14} cm^{-3}), the largest differences between our atom and the SH results are 2%. The largest disagreements are caused by differences in the rate coefficients for collisional excitation and ionization of higher levels. Tests are also presented in FF that

show that collisions from the ground term and line trapping change the actual emission substantially away from simple theory for densities appropriate for quasar clouds.

Unpublished tests show that factors of 2 changes in the collisional rates for levels $n > 3$, roughly the uncertainty in the atomic data, result in changes in line intensities by $\sim 10\%$ at nebular temperatures and intermediate densities ($\sim 10^8 \text{ cm}^{-3}$). They change by less at lower densities and by more at very high densities and low temperatures. Similar uncertainties affect rate coefficients for collisional ionization from excited states. These (together with the radiative transfer issues discussed below) are a fundamental uncertainty in predicting theoretical intensities.

2.5. Free-Free Emission and Absorption

Thermally averaged free-free Gaunt factors are calculated via a two-dimensional Chebyshev expansion given by Hummer (1988). The fit is valid over a wide range in frequency and temperature, $-4.0 < \log(h\nu/kT) < 1.5$ and $-3.0 < \log(Z^2 \text{ ryd}/kT) < 3$. CLOUDY, however, uses a much broader set of energies. Rather than extrapolating the Hummer formulae, we have instead matched the asymptotic equations given in Rybicki & Lightman (1979) to the Hummer results. This approach avoids dangerous extrapolation and retains the basic physics of the gas in extreme conditions.

Figure 1 shows the results of the computations just described, which result in a very smooth function of temperature and photon energy. In the figure we have highlighted those points that come from Hummer's (1988) fits. In some cases the Hummer results did not really extend to regimes in which the asymptotic results were valid. In these cases, the asymptotic formulae and the fits of Hummer, or even the asymptotic formulae themselves, do not match well at the boundaries. In such circumstances we have interpolated in order to avoid any discontinuities. There is a clear need for future work giving accurate Gaunt factors over the full energy range.

3. HELIUM

3.1. Structure of the Model Atoms

Helium is treated as three separate atoms/ions, with the ion and singlets each a 10-level atom, and the triplets a five-level atom. Like the hydrogen atom, the helium ion and singlets in C84 were based on the work of Cota (1987) and suffered similar problems when exposed to intense nonthermal radiation fields. The atoms have been changed so that all levels represent actual levels, and the highest level is assigned the recombination coefficient corresponding to the integral from 9 to infinity. Because of the l -mixed assumption, the emissivity of the helium atom/ion will have the same limitations that were true of hydrogen before C90—the He II and He I singlet atoms do reproduce the intensities in the well l -mixed high-density limit but are not valid in the low-density limit. The code also predicts simple Case B intensities, which should be used under nebular

conditions. The triplets resolve l -states and are close to exact predictions for all conditions.

Extending the model helium atom and ion to a generalized structure similar to the current hydrogen atom will be a high priority in the coming years.

The photoionization cross sections for atomic helium are now based on accurate fits to experimental values (Samson et al. 1994) given by Verner et al. (1996a). These are significantly different at high energies from those given by Brown & Mathews (1970), which were used in C84. This has had some impact on the ionization structure of clouds exposed to hard radiation fields. The newer cross sections are expected to be nearly exact.

3.2. Collision Data

We have undertaken a major effort to update the collision data for helium.

3.2.1. Helium Atom

The He^0 ground-state collisional ionization data are from Voronov (1997). For the excited singlet states we use hydrogenic cross sections since we could not find better. For the He^0 2^3S and 2^3P triplet states, collisional ionization rates are from Seaton (1964). We know of no rates for higher lying triplet states.

For de-excitation rates between the low-lying levels ($1s$ – $2s$, $2p$, and $2s$ – $2p$) of the He^0 singlets, we use the data of Sawey & Berrington (1993). Hydrogenic rates are used for collisions involving the ground or first excited states and the highly excited states ($n > 3$). For rates between the highly excited states, we use the analytic expressions of Vriens & Smeets (1980) for hydrogen. For collisional de-excitation rates involving the triplet states, we again use the data from Sawey & Berrington (1993). We also include collisions involving the $2s$, $2p$ triplet and the $1s$ and $2s$, $2p$ singlet states, again using the data from Sawey & Berrington.

3.2.2. Helium Ion

We now use Voronov (1997) for collisional ionization from the ground state of He^+ and for excited states use the analytical expressions of Seaton (1962) and Bely & Van Regemorter (1970) at low temperatures and Sampson & Zhang (1988) at high temperatures. Collisions between the $1s$, $2s$, $2p$, and 3 states (excluding the $2s$ – $2p$ transition) are from Aggarwal et al. (1992) and for higher excited states are from Sampson & Zhang (1988). Proton and electron collision rates between $2s$ and $2p$ are taken from Zygelman & Dalgarno (1987).

4. THE HEAVY ELEMENTS

4.1. Elements and Abundances

C84 included the 13 elements H, He, C, N, O, Ne, Na, Al, Si, S, Ar, Fe, and Ni. All stages of the 30 lightest elements,

H–Zn, are now included. The default set of abundances is from Grevesse & Anders (1989) and Grevesse & Noels (1993). The biggest difference between this and those used in C84 is in the iron abundance, now about 70% of the former value. This reflects the difference between solar meteoritic and photospheric abundances. Hazy lists the specific abundances in both number density and mass fractions.

4.2. Ionization Processes

4.2.1. Heavy-Element Photoionization Rates

Our implementation for the evaluation of the photoionization rates for heavy elements follows Verner & Yakovlev (1995), with extensions to more recent Opacity Project (OP) data (Verner et al. 1996a). The photoionization rate, heating rate, and photoelectron yield are evaluated independently for each electronic subshell. There are a total of seven possible subshells for the heaviest elements. We now take fluorescence yields for each subshell from electronic forms of the tables of Kaastra & Mewe (1993).

Figure 2 shows an example for atomic iron. Partial photoionization cross sections are indicated (from Verner et al. 1996a), along with the distribution of photoelectrons that result (from Kaastra & Mewe 1993). It has only now become possible to treat every subshell separately, thanks to the speed of modern workstations. This is a major time sink and is the main reason that calculations with the current version now take significantly longer than calculations did with C84.

Suprathermal Auger electrons often have sufficient energies to produce further collisional ionizations before they are thermalized. We now use efficiencies from Xu & McCray (1991). C84 used formulae from Shull & van Steenberg (1985) that did not go to the proper asymptote in the low electron fraction limit. This causes small changes in the heating and ionization efficiency for very neutral gas.

4.2.2. Photoionization Cross Sections

Photoionization cross sections are now generated with the routine PHFIT (Verner & Yakovlev 1995; Verner et al. 1996a). This uses a mix of experimental and theoretical (including Opacity Project) sources to generate cross sections, subshell by subshell. In particular Verner et al. (1996a) use the most recent results from the Iron Project (Hummer et al. 1993; Nahar & Pradhan 1994; Bautista & Pradhan 1995) for the ions they calculated. The fits average over sharp resonances and do not try to fit them. This is appropriate because the position of most resonances is uncertain by a factor that is well more than their width. For the majority of the species, the photoionization cross sections are accurate to better than 10%, although this is somewhat worse for closed shells such as Ar or Ne. The fits are extrapolated to 100 MeV, needed by CLOUDY but well beyond the original cross section calculations, and this is an additional uncertainty. However, in practice, photons above 50 keV have

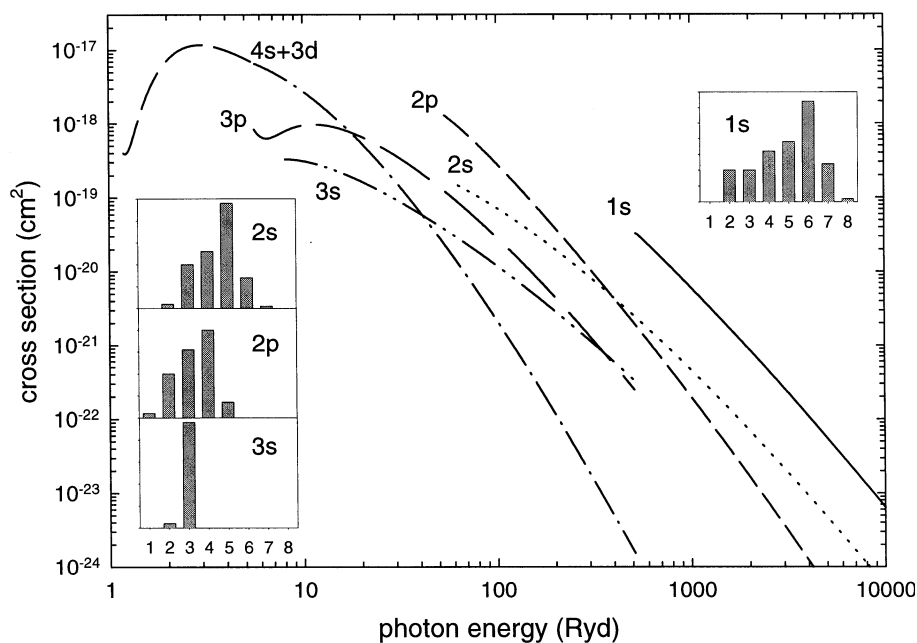


FIG. 2.—Iron photoionization cross sections. Partial cross sections for each subshell are shown, along with the shower of Auger electrons that is produced.

little effect on the ionization or thermal balance because of the small photoelectric cross section.

These cross sections are largely similar to the Reilman & Manson (1979) values, which were used by C84, for moderately and highly ionized species. The methods used by Reilman & Manson became increasingly approximate for smaller charge, and the new cross sections are often significantly larger for atoms and first ions. Verner et al. (1996a) lists those elements for which the current photoionization cross sections differ from Reilman & Manson. For some species, including O^+ and most neutral atoms and single ions of the third and fourth row, the results can be quite different, and this has had a moderate effect on some ionization fractions. The biggest resulting differences between C84 and C90 have been changes in the predicted $O\text{ III}/O\text{ II}$ ratios and in the intensities of $[Ca\text{ II}]$ lines, owing to changes in the O^+ and Ca^+ cross sections.

PHFIT is continuously updated as the theoretical and experimental photoionization database expands, and this updated version is available from the Web site.

4.2.3. Auger Yields

Fluorescent yields are now taken from the Kaastra & Mewe (1993) tabulation of multielectron rates for each subshell of the first 30 elements. These results are available in numerical form and should be quite accurate. The code iterates on the ionization distribution to include multielectron processes while keeping the matrix bidiagonal. These results differ considerably from the approach used in C84, taken from Weisheit & Dalgarno (1972), Weisheit (1974), and Weisheit & Collins (1976). This results in significant differences in the predicted ionization dis-

tribution of third-row and higher elements when ionized by very hard X-ray continua (typical energies of several keV).

4.2.4. Excited State Photoionization

Deep within a cloud the radiation field can be heavily extinguished at energies above strong ionization edges, such as those of H^0 , He^0 , or He^+ . For species with ground terms shielded by these edges, the dominant ionization channel can be photoionization from excited states with ionization potentials below these edges. Classical examples (see Swings & Struve 1940) are photoionization from O^{2+} (the ground is shielded by He^+) and N^0 and Mg^+ (shielded by H^0).

Figure 3 shows an example of this shielding deep within a quasar cloud. This is the lower density ($n_H = 10^{10}\text{ cm}^{-3}$) model of Table 1 of Rees, Netzer, & Ferland (1989). The local continuum is plotted at a point 10^{22} cm^{-2} from the illuminated face, a point near maximum production of $Mg\text{ II } \lambda 2798$. For BLR clouds the predicted $Mg\text{ II}$ intensity can differ by as much as 30% between C84 and C90 owing to changes in the cross section for Mg^+ excited state photoionization. The code now uses OP data for all excited levels but had previously used screened hydrogenic estimates for many.

4.2.5. Collisional Ionization

Rate coefficients for collisional ionization from the ground states of the first 28 elements are compiled and fitted by Voronov (1997). We extrapolated them for minor elements 29 and 30. These have been into Verner's routine CFIT, which is available from the ADfA Web site.

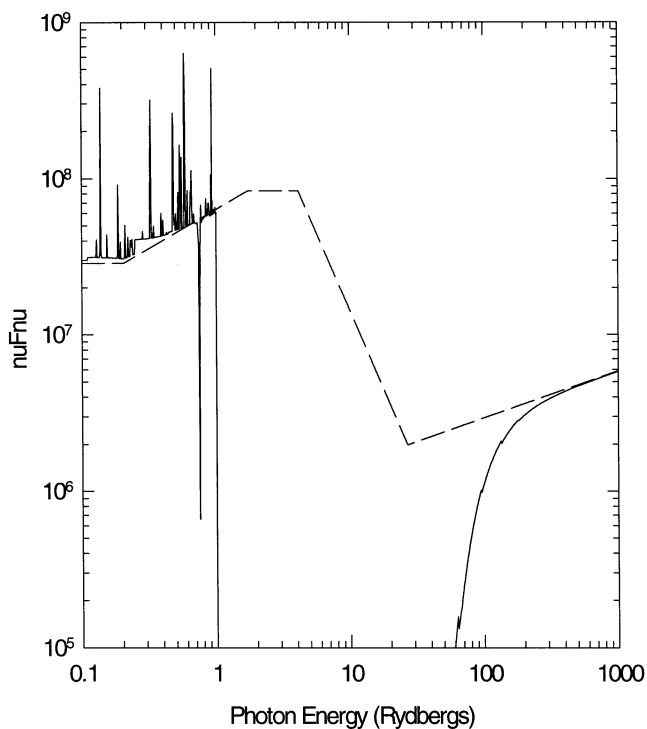


FIG. 3.—Incident continuum (*dashed line*) and local continuum at a column depth of 10^{22} cm^{-2} into the 10^{10} cm^{-3} model presented in Table 1 of Rees et al. (1989). The continuum above 1 ryd is heavily extinguished, so photoionization from excited states that lie below 1 ryd is an effective photon destruction mechanism.

4.3. Recombination Processes

A photoionization database is of only academic value unless it is matched with a self-consistent set of recombination rate coefficients. The predicted ionization balance would violate the approach to thermodynamic equilibrium were this not the case. Furthermore, the fact that self-consistent photoionization cross sections and recombination rates go up or down together make the ionization balance less sensitive to detailed cross sections than one would otherwise imagine.

The total electron-ion recombination process involves three distinct physical channels: radiative, low-temperature dielectronic, and high-temperature dielectronic recombination. Two limiting situations, collisional and photoionization equilibria, are found in nature. In collisional equilibrium, temperatures kT are about equal to the ionization energy of the species, while in photoionization equilibrium, kT is much less than the ionization energy. Radiative recombination can be significant at any temperature, low-temperature dielectronic recombination usually dominates in photoionization equilibrium, and high-temperature dielectronic recombination dominates at collisional temperatures.

4.3.1. Radiative Recombination Rates

We have calculated radiative recombination rates for recombination to all H-like, He-like, Li-like, and Na-like ions of

elements from H through Zn and have fitted them with analytical formulae (Verner & Ferland 1996). For these cases the parent ion is a closed shell, and autoionizing levels are not expected to occur close to the ionization threshold. Radiative recombination should dominate for most temperatures for these ions. The only significant uncertainty is in the photoionization cross sections, which should be known to better than 15%. The recombination coefficients should be this accurate. A routine (RRFIT) to calculate these rates is available on the ADfA Web site.

Radiative recombination rate coefficients can be obtained to this accuracy for all species. Unfortunately, for those species not considered by Verner & Ferland (1996), the recombination process is dominated by the other, far more uncertain, mechanisms described next.

4.3.2. Low-Temperature Dielectronic Recombination

Nussbaumer & Storey (1983, 1984, 1986, 1987; hereafter NS83, NS84, NS86, and NS87) calculated low-temperature dielectronic recombination rates for some ions of C, N, O, Ne, Mg, Al, and Si using available experimental data on energies of autoionizing levels. This is a process that occurs through low-lying autoionizing stages. This is usually an important, often dominant, recombination process for those species whose parent ions do not have closed shells.

Uncertainties in energies of the autoionizing resonances are crucial. In the usual case, the autoionizing levels are assumed to be in LTE with the continuum, owing to rapid dielectronic recombination/autoionization. The recombination rate is then the population of the level multiplied by its rate of decay to bound levels. This population depends on the Boltzmann factor and so depends exponentially on the energies of these levels. It will be difficult to improve upon NS83, NS84, NS86, and NS87 since they did all species with accurate experimental energies.

Within the framework used by Nussbaumer & Storey in this series of papers, there is a further uncertainty regarding which autoionizing levels will be in LTE with the continuum. Levels with many spins exist, but only those in which the spin changes by 1 are connected by an allowed transition in the continuum. Only these levels were included in the early papers in the Nussbaumer & Storey series. In later papers two rates were given for the two cases, one with only directly connected levels included, and another with all possible levels. The rates differ by a factor of 2 in some cases.

The lack of reliable dielectronic rate coefficients for most third-row and higher elements is the dominant uncertainty in the ionization balance in photoionization equilibrium. Most ions do not have complete spectroscopy and measured autoionization levels. Theoretical structure calculations can be done, but uncertainties in the positions of the resonances remain. The question concerning populations of levels not coupled by an *LS*-allowed transition to the continuum is central. This is likely

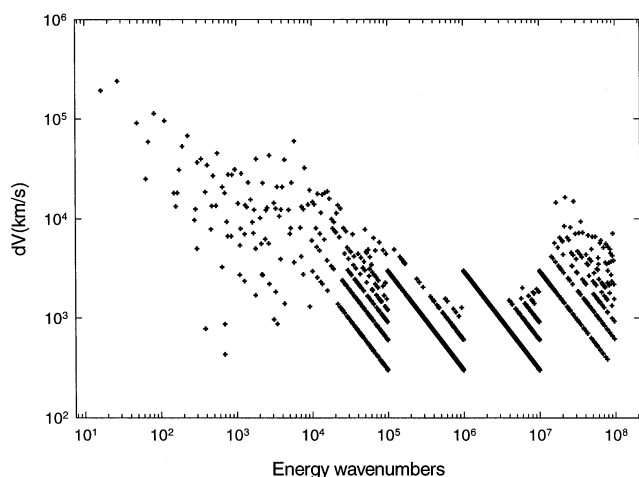


FIG. 4.—Velocity separation between neighboring lines for all lines now in the code. The lines do not begin to overlap until line widths of several hundreds of km s^{-1} are reached. When this happens, the approximation of treating each line individually begins to break down.

to remain an uncertainty for some time to come and points to the need for complete basic experimental data.

For third-row or heavier elements, our choice is either to assume zero for the uncalculated rates or to use guesses based on the charge of the species and second-row rates (Ali et al. 1991). We have taken this latter approach as the default condition, but it is easy to allow zero or an arbitrary rate to be taken instead. This affects intensities of some lines (especially the [S II] $\lambda\lambda 6716, 6731$ doublet) by as much as a factor of 2.

4.3.3. High-Temperature Dielectronic Recombination

We use published fits for high-temperature dielectronic recombination (HTDR) rates based on calculations made in the low-density limit (Aldrovandi & Pequignot 1972, 1974; Shull & Van Steenberg 1982; Arnaud & Rothenflug 1985; Arnaud & Raymond 1992). This process mainly affects gas in collisional, not photoionization, equilibrium because it is efficient when the electron energy approaches the ionization potential of the species. These rates are largely based on the Burgess (1965) formula. Where detailed calculations have been made (Badnell 1991; Savin et al. 1997), rates have been only within 0.5 dex of the Burgess estimate. The Burgess formula seems to overestimate the more accurate rates. This remains a major uncertainty.

High-temperature dielectronic rates are significantly suppressed at moderate to high densities, $>10^{10} \text{ cm}^{-3}$ (Davidson 1975). We use the original form of the Davidson approximation to take suppression into account for all species and densities. The form of the density dependence is not generally known in detail and represents another uncertainty. Our fit to the David-

son calculations gives a suppression factor of

$$\max\left(0.08, \min\left\{1, 1 - 0.092 \log\left[\frac{n_e}{(z/3)^7 \sqrt{T/15,000}}\right]\right\}\right). \quad (1)$$

In this equation, z is the charge of the ion before recombination, T is the electron temperature, and n_e is the electron density.

4.3.4. Charge Exchange

All neutralization and ionization reactions between hydrogen and the first four ions of all species are included using the fits listed by Kingdon & Ferland (1996) and Ferland et al. (1997). Charge transfer between heavy elements and helium are from a variety of sources. The numerical form of the rates, and a routine to calculate them, is available from the ADfA Web site as routine HCTRecom (hydrogen charge transfer recombination) and HCTIon (ionization).

4.4. Resulting Ionization Balance

As a test of the internal consistency of the resulting ionization balance, we have performed two sets of tests, using CLOUDY and LineSpec (Verner & Yakovlev 1990). The second code is designed to determine ionization balance for collisional or photoionization equilibrium for an optically thin constant temperature gas. These independently developed codes are in excellent agreement.

4.5. Emission Lines

The increase in the number of elements included has allowed us to make a major extension to the number of emission lines treated in the code. The current version of the code predicts intensities of $\sim 10^4$ lines from the 30 elements.

The lines are divided into two groups. The level 1 lines have accurate wavelengths and quantal calculations of the collision strengths. There are several hundred lines that fall into this category, and these include most of the strongest lines. For these cases we have created temperature-dependent fits to individual collision strengths. Level 2 lines have Opacity Project wavelengths (typically accurate to roughly 10%) and use g-bar approximation collision strengths. Collision strengths determine the rate atoms are excited, so level 2 lines have intensities that are uncertain by as much as the g-bar approximation (Gaetz & Salpeter 1983; Mewe 1972; van Regemorter 1962). This can easily be 0.5 dex. Level 2 lines are, unfortunately, the majority of the lines.

Lines are largely computed as distinct entities, with background opacity due to the computed continuum. This approximation is valid only when the density of lines is low, but this is the case for resonance lines. Figure 4 shows the velocity separation between neighboring lines for all lines in our resonance line list. Typical separation is hundreds of kilometers

per second. Lines would merge if the turbulent line width were large or if subordinate lines were optically thick (since the density of these lines is so great). Subordinate lines will become optically thick when they approach LTE at densities greater than 10^{14} cm^{-3} . This approximation establishes one end of the range of validity of the code. The solution is to make the continuum mesh fine enough to resolve all lines well and then fully transfer this continuum. Today this approach would require prohibitive execution times and would make a difference only at densities high enough for subordinate lines to be optically thick.

4.5.1. Line Excitation, Heating-Cooling, and Intensity

Collisional excitation, de-excitation, line escape, and continuum pumping are included as excitation mechanisms for all lines. The entire treatment of line heating and cooling has undergone a major revision since the code is now often used to simulate gas with heavily enhanced abundances (Hamann & Ferland 1993; Ferland et al. 1996).

Continuum pumping from the upper to lower level, owing to the attenuated incident continuum, has a rate (Ferland & Rees 1988; Rees et al. 1989; Ferland 1992) given by

$$\gamma_{u,l} = A_{u,l} \eta \text{ s}^{-1}, \quad (2)$$

where η is the dimensionless occupation number of the attenuated incident continuum. This occupation number is evaluated by attenuating the incident continuum by the continuous photoelectric opacity of the gas and then applying an escape probability-like correction for the probability that a continuum photon will penetrate to the current line optical depth (see Ferland 1992). This is in keeping with the assumption outlined in the previous section, that lines are largely independent of one another. The backward rate, the rate at which the attenuated incident continuum excites the transition, is given by

$$\gamma_{l,u} = \gamma_{u,l} \frac{g_u}{g_l} = A_{u,l} \eta \frac{g_u}{g_l} \text{ s}^{-1}, \quad (3)$$

where the g 's are the statistical weights. Then, the balance equation for a two-level atom is

$$n_u (c_{l,u} + \gamma_{l,u}) = n_u [c_{u,l} + A_{u,l} (\varepsilon + \gamma_{u,l})], \quad (4)$$

where $c_{l,u}$ is the collision rate (units s^{-1} and is equal to $q_{l,u} n_e$, where $q_{l,u}$ is the excitation rate coefficient and n_e is the electron density), ε is the escape probability, and γ is the pumping rate.

The local volume intensity of the line, produced locally and

escaping the cloud, is

$$4\pi j = n_u A_{u,l} \varepsilon h\nu \text{ ergs cm}^{-3} \text{ s}^{-1}, \quad (5)$$

while the net cooling per unit volume is

$$\Lambda = (n_l c_{l,u} - n_u c_{u,l}) h\nu \text{ ergs cm}^{-3} \text{ s}^{-1}. \quad (6)$$

With these definitions it is clear how exposure to an external continuum can drive a gas with many lines into thermal equilibrium with that radiation field. We can define a relative level departure coefficient as

$$b_u = (n_u/n_l) / (n_u/n_l)^*, \quad (7)$$

where the quantity with the asterisk is the value in thermodynamic equilibrium,

$$(n_u/n_l)^* = g_u/g_l \exp(-h\nu/kT), \quad (8)$$

and in detailed balance

$$c_{l,u} = (n_u/n_l)^* c_{u,l}. \quad (9)$$

Then equation (6) can be rewritten as

$$\Lambda = n_l c_{l,u} (1 - b_u) h\nu \text{ ergs cm}^{-3} \text{ s}^{-1}. \quad (10)$$

Thus a line will heat rather than cool the gas if the departure coefficient is greater than 1. When the line comes into LTE ($b = 1$), it has no thermal effect.

Pumping by the external continuum can be a significant heating source even when the brightness temperature of the continuum is well below the local electron temperature. Comparing cases with and without the external continuum, there will be significant extra heating when the continuum pumping rate excitation term approaches the collisional excitation term, $c_{l,u}$. This heating is of order

$$G \approx \gamma_{l,u} c_{l,u} / (c_{u,l} + A_{u,l}) h\nu \text{ ergs cm}^{-3} \text{ s}^{-1}. \quad (11)$$

Energy exchange between two levels will be a net heating or cooling source if the level populations are out of LTE. The energy balance is given by

$$\Lambda_{\text{net}} = \Lambda - G = (n_l c_{l,u} - n_u c_{u,l}) h\nu \text{ ergs cm}^{-3} \text{ s}^{-1}. \quad (12)$$

If we express the upper to lower level populations as a departure

coefficient relative to ground, then

$$n_u = b_u n_l \frac{g_u}{g_l} \exp(-h\nu/kT) \quad (13)$$

and

$$\Lambda_{\text{net}} = n_l [c_{l,u} - b_u c_{u,l} \exp(-h\nu/kT)] h\nu \text{ ergs cm}^{-3} \text{ s}^{-1}. \quad (14)$$

Since $c_{l,u}$ and $c_{u,l}$ are related by $c_{l,u} = c_{u,l} \exp(-h\nu/kT) g_u/g_l$, we obtain, in the end,

$$\Lambda_{\text{net}} = n_l \exp(-h\nu/kT) c_{l,u} (1 - b_u) h\nu \text{ ergs cm}^{-3} \text{ s}^{-1}. \quad (15)$$

A level will cool if the upper population is below its LTE value and will heat if it is above. The Einstein coefficients ensure that irradiation by a true blackbody will drive the level populations to LTE. This is the physics that ensures that the high-metallicity clouds equilibrate at the continuum temperature. In the limit in which lines dominate the heating and cooling, they will ensure that the gas temperature equilibrates at the radiation temperature of the incident radiation field. A test case discussed below shows that this is indeed the case.

4.5.2. The Emission-Line List and Database

The *entire* atomic database has been revised in C90. A list of references to the current data is given in Table 1. The transition probabilities for lines of C, N, and O come from the Opacity Project data and the new NIST compendium (Verner, Verner, & Ferland 1996b; Wiese, Fuhr, & Deters 1996). Great care has gone into implementing this data set. As an example, the [O III] $\lambda 5007$ line has a transition probability of $1.8135 \times 10^{-2} \text{ s}^{-1}$, and $\lambda 4959$ has $A = 6.215 \times 10^{-3} \text{ s}^{-1}$. The ratio is 2.918, and this is the ratio of photons. The ratio of energies is this times $\lambda 4959/\lambda 5007$, or 2.89, the answer the code gets. In *LS* coupling, the ratio of transition probabilities should be the ratio of statistical weights, or 3, since the lines have the same upper level. Quantal calculations do not obtain this ratio exactly, however.

4.6. Molecule Network

The code includes the heavy-element molecule network given by Hollenbach & McKee (1989; Ferland, Fabian, & Johnstone 1994 discuss this). The hydrogen network is described both there and in Ferland & Persson (1989). This has not been an area of active development in recent years, since environments that are predominantly molecular are seldom time-steady (Bertoldi & Draine 1996). The current emphasis in developing the code is to obtain the best possible simulation in the time-steady case.

TABLE 1
ATOMIC DATA REFERENCES FOR THE DATABASE
NOW INSIDE CLOUDY

Number	Source
1	Aggarwal 1983a
2	Aggarwal 1983b
3	Aggarwal 1984
4	Aggarwal 1985
5	Aggarwal et al. 1992
6	Allard et al. 1990
7	Baluja 1985
8	Baluja & Zeippen 1988
9	Berrington 1985
10	Berrington 1988
11	Berrington et al. 1985
12	Bhatia & Doscheck 1995
13	Bhatia & Mason 1986
14	Blum & Pradhan 1992
15	Brage, Froese Fischer, & Judge 1995
16	Brage, Hibbert, & Leckrone 1997
17	Brage, Judge, & Brekke 1996
18	Burke, Lennon, & Seaton 1989
19	Butler & Zeippen 1984
20	Butler & Zeippen 1994
21	Butler & Dalgarno 1980
22	Calamai & Johnson 1991
23	Calamai, Smith, & Bergeson 1993
24	Callaway 1994
25	Callaway, Unnikrishnan, & Oza 1987
26	Chandra 1982
27	Chidichimo 1981
28	Cochrane & McWhirter 1983
29	Dopita, Mason, & Robb 1976
30	Dufton et al. 1986a
31	Dufton, Doyle, & Kingston 1979
32	Dufton et al. 1986b
33	Dufton et al. 1982
34	Dufton & Kingston 1984
35	Dufton & Kingston 1987
36	Dufton & Kingston 1989
37	Dufton & Kingston 1991
38	Dufton & Kingston 1994
39	Dumont & Mathez 1981
40	Fang & Kwong 1997
41	Federman & Shipsey 1983
42	Fleming et al. 1996
43	Fleming et al. 1995
44	Flower 1976
45	Froese Fischer 1983
46	Froese Fischer 1995
47	Galavis, Mendoza, & Zeippen 1995
48	Garstang 1957
49	Garstang, Robb, & Rountree 1978
50	Giles 1981
51	Hayes 1986
52	Hibbert, Godefroid, & Froese Fischer 1995
53	Ho & Henry 1984
54	Hummer & Storey 1987
55	Johansson et al. 1995
56	Johnson, Burke, & Kingston 1987
57	Johnson, Kingston, & Dufton 1986
58	Kafatos & Lynch 1980
59	Kaufman & Sugar 1986

TABLE 1
(CONTINUED)

Number	Source
60	Keenan & Norrington 1987
61	Keenan et al. 1992
62	Kingston 1986
63	Krueger & Czyzak 1970
64	Kwong et al. 1993
65	Leep & Gallagher 1976
66	Lennon & Burke 1991
67	Lennon & Burke 1994
68	Lennon et al. 1985
69	Lepp & Shull 1983
70	Mason 1975
71	McLaughlin & Bell 1993
72	Mendoza 1982
73	Mendoza & Zeppen 1982a
74	Mendoza & Zeppen 1982b
75	Mendoza & Zeppen 1983
76	Mendoza & Zeppen 1987
77	G. Merkelis, M. J. Vilkas, G. Gaigalas, & R. Kisielius 1994, private communication
78	Mohan, Hibbert, & Kingston 1994
79	Muhlethaler & Nussbaumer 1976
80	Neufeld & Dalgarno 1987
81	Nussbaumer 1986
82	Nussbaumer & Rusca 1979
83	Nussbaumer & Storey 1981
84	Nussbaumer & Storey 1982
85	Nussbaumer & Storey 1988
86	Oliva, Pasquali, & Reconditi 1996
87	Pelan & Berrington 1995
88	Ramsbottom & Bell 1997
89	Ramsbottom, Bell, & Keenan 1997
90	Ramsbottom, Bell, & Stafford 1996
91	Ramsbottom, Berrington, & Bell 1995
92	Ramsbottom et al. 1994
93	Saha & Trefftz 1982
94	Saha & Trefftz 1983
95	Sampson & Zhang 1988
96	Saraph 1970
97	Saraph & Storey 1996
98	Saraph, Storey, & Tully 1995
99	Saraph & Tully 1994
100	Sawey & Berrington 1993
101	Seaton 1964
102	Sigut & Pradhan 1995
103	Stafford et al. 1994
104	Stafford, Hibbert, & Bell 1993
105	Stepney & Guilbert 1983
106	Storey, Mason, & Saraph 1996 (http://adc.gsfc.nasa.gov/adc-cgi/cat.pl?/catalogs/6/6064/)
107	Sugar & Corliss 1985
108	Tayal 1997
109	Tayal, Burke, & Kingston 1985
110	Tayal & Henry 1986
111	Tayal, Henry, & Pradhan 1987
112	Tielens & Hollenbach 1985
113	Wahlgren 1995
114	Wiese, Fuhr, & Deters 1996
115	Wills, Wills, & Netzer 1985
116	Wills & Netzer 1979
117	Zeppen 1982

TABLE 1
(CONTINUED)

Number	Source
118	Zeppen 1990
119	Zeppen, Le Bourlot, & Butler 1987
120	Zhang, Graziani, & Pradhan 1994
121	Zygelman & Dalgarno 1987
122	Zygelman & Dalgarno 1990

5. THERMAL BALANCE

This section shows two sample calculations that illustrate the effects of line heating and cooling on the equilibrium temperature.

5.1. Thermodynamic Equilibrium of High-Metallicity Gas

Figure 5 shows the results of a series of calculations for a gas strongly enriched in heavy elements, corresponding to $Z = 10Z$ using the abundance grid described by Hamann & Ferland (1993). This metallicity is large enough for hydrogen to be a relatively minor constituent. The gas is exposed to a radiation field with a blackbody shape corresponding to several color temperatures and various values of the energy density temperature for each color temperature. Ferland & Rees (1988) and Ferland & Persson (1989) gave analogous calculations for pure hydrogen clouds. This example tests both the ionization and thermal balance in an extreme environment in which the heavy elements totally dominate the situation.

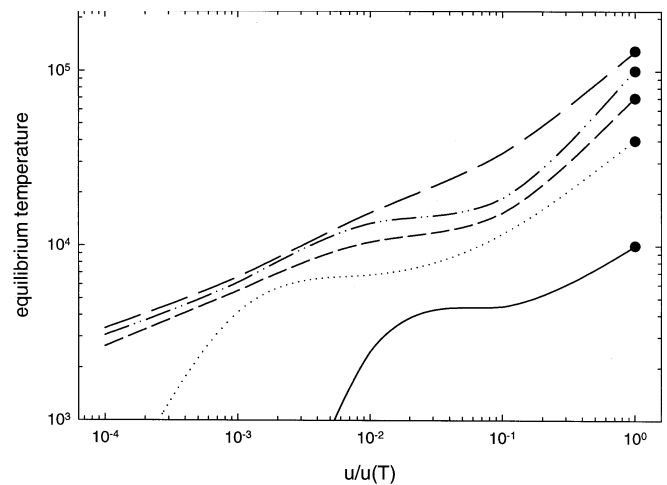


FIG. 5.—Equilibrium temperature of gas exposed to five blackbodies with various energy density temperatures. The color temperatures of the blackbodies are 10,000, 40,000, 70,000, 100,000, and 130,000 K. The metallicity was 10 times solar (Hamann & Ferland 1993) so that heating and cooling of thousands of heavy-element emission lines dominates the thermal equilibrium. The simulation is of an optically thin cell of gas with density 10^{10} cm^{-3} (results do not depend on this density). The x -axis is the local energy density relative to the energy density in thermodynamic equilibrium at that temperature. The gas goes to thermodynamic equilibrium when the radiation field does (the color and energy density temperatures are equal).

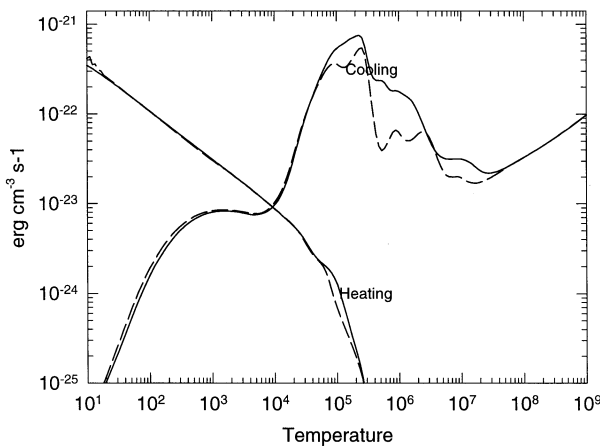


FIG. 6.—Cooling function for low-density gas under conditions of collisional ionization. Results from the current version of the code are shown as the solid line, while those from C84 are shown as the dashed line. Peaks are now far broader, the result of so many lines in the cooling function.

The energy density temperature relative to the blackbody color temperature is shown as the x -axis. The filled circles represent the cases in which the energy densities and the color temperature of the radiation field are equal and strict thermodynamic equilibrium is expected. The figure shows that this is indeed the case.

The gas temperature goes to the color temperature because of induced transitions between the 10^4 lines in the cooling function. The distribution of ionization for each color temperature is radically different, but the line interactions with this field bring the gas to the expected equilibrium temperature.

The lowest temperature we can obtain true equilibrium with the current version of the code is about 4000 K, owing to the formation of molecules. This is because our treatment of molecular cooling is based on fits to published cooling curves and does not include the detailed microphysics described above. We expect to extend the molecular cooling calculations to a more formal footing in the near future.

5.2. Cooling Function for Low-Density Gas

Figure 6 compares cooling rates computed by the current version of the code compared with C84 for a purely collisionally ionized solar abundance gas at various temperatures. The presence or absence of bumps affects the thermal stability of the gas, since local minima can provide local patches of stable equilibrium. The total cooling near the broad 10^6 K peak is now more featureless. This is due to the presence of many more elements and the many cooling lines they contribute. The sharper peaks in the older calculations were dominated by cooling by a few lines. These details are also affected by abundances—in particular, the iron abundance we now use is somewhat lower.

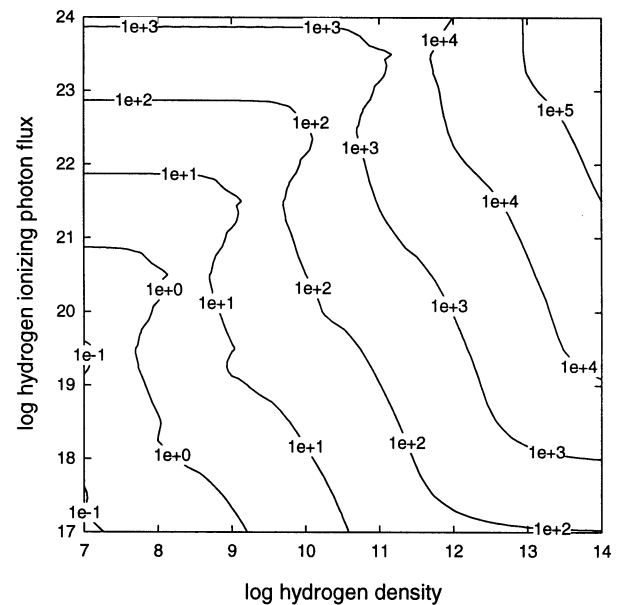
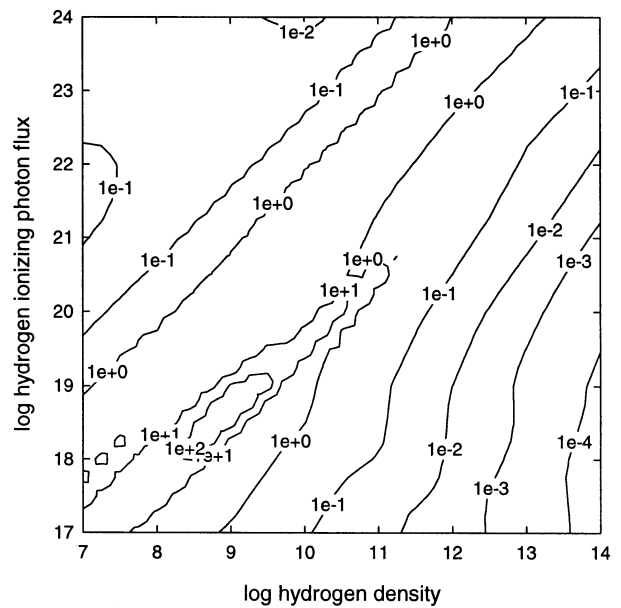


FIG. 7.—Ratio of maximum radiation to gas pressure (dyn cm^{-2} ; top) and greatest radiative acceleration at illuminated face (cm s^{-2} ; bottom) for solar abundance BLR clouds exposed to the Mathews & Ferland (1987) continuum.

5.3. Dynamics of Quasar Broad-Line Region Clouds

Pressure due to trapped lines (Elitzur & Ferland 1986) and radiative acceleration due to absorption of the incident continuum (Baldwin et al. 1996) are now computed for all lines. This is a major increase in the number of transitions—C84 included this physics for only a few dozen lines. Figure 7 shows the results. The effect of many thousands of resonance lines produces a dramatic increase in the total radiation pressure. A large fraction of the clouds would not be stable against radiation

pressure if they were supported by external pressure (Elitzur & Ferland 1986 discuss this instability), and radiation pressure due to the incident continuum could drive mass loss even from main-sequence stars. This has implications for the origin of the emitting gas in quasars since mechanisms exist for driving mass loss.

6. RELIABILITY IN THE FACE OF COMPLEXITY

There are three sources of uncertainty in any large-scale numerical simulation: bugs, the numerical methods employed, and the basic atomic data. The code now consists of well over 10^5 lines of FORTRAN and is used to simulate environments in which analytical solutions are not possible. Anything as complex as CLOUDY certainly contains errors. The fact that analytical solutions are not possible makes it difficult to validate a simulation. As machines grow ever faster and codes more complex, finding validation methods will become a core problem in any numerical endeavor. This section outlines the methods we have developed to try to get the right answer.

6.1. Coding Methods

The coding methods now being used in the development of CLOUDY have been strongly influenced by those developed at Microsoft (McGuire 1993). The basic idea is never to solve the same problem twice. Whenever any problem is encountered, new code is embedded to check that this never happens again. Examples include negative electron temperatures or collision strengths. These tests are often redundant and do slow the code slightly, so they are bracketed by comments that make it possible to remove them automatically. These tests are so extensive that it is now common for newly introduced problems to be detected automatically.

6.2. CLOUDY's Stability

A major use of spectral synthesis calculations is to deduce the conditions and abundances in the matter producing a spectrum. There is always a question of uniqueness since there may be more than one way to get any particular result, and we must work backward to deduce the question (properties of the object) from the answer (the emitted spectrum). Examining predictions over the very broadest possible range of physical parameters is vital to really understand what a spectrum is telling us.

Today the code is often used to generate very large grids, involving thousands of complete simulations, to generate contour or three-dimensional plots like that shown in Figure 8. This is an example, based on Baldwin et al. (1995), which shows that one of the strongest quasar emission lines is most efficiently produced over a very narrow range of conditions. The peak visibility occurs for the parameters long ago deduced as "standard" quasar conditions. We argued that this is likely just a selection effect.

A major effort has gone into making it possible to generate

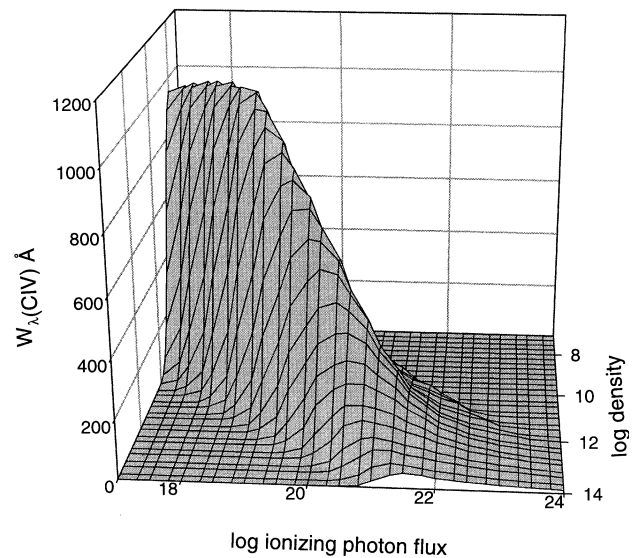


FIG. 8.—C IV $\lambda 1549$ equivalent width for a wide range of densities and flux of photons.

such large grids on a routine basis. Some of the issues include the following:

1. The code must have enough intelligence to converge models autonomously with very different conditions, without user intervention. This goal has largely been realized. All of the predictions shown here are the result of fully autonomous calculations with no outside intervention.

2. The code must respond appropriately no matter what boundary conditions are set. It goes to the Compton, molecular, ISM, and LTE limits. The temperature limits are $2.8 \text{ K} < T < 10^9 \text{ K}$. The high-temperature limit is set by the assumption that electrons are nonrelativistic. The density limits are $10^{-5} \text{ cm}^{-3} < n(\text{H}) < 10^{14} \text{ cm}^{-3}$. The low-density limit is set by the exponential range of IEEE 32-bit machines, and the high-density limit is set because of the approximate treatment of line transfer and since most ions are treated as two-level systems. Densities as high as 10^{16} cm^{-3} can be treated with less accuracy. The code will identify conditions that are inappropriate for its use.

3. The code must examine its results and predictions to confirm that the simulation is valid. It simply is not possible to go over the many tens of megabytes of results generated in large grids, after the fact, to confirm that all went well. As the code is developed, potential problems are identified and logic is added to check for this in future calculations.

The code *will probably* converge a simulation with no problems, and it *will certainly* identify any problems at the end of the calculation. These are essential core features, vital if very large grids are to be computed reliably. Each simulation ends with a summary of all remarkable or surprising features, an analysis of any convergence problems, and checks that the range of validity was not exceeded. One specific example of

these internal checks is that the code now tracks timescales for all heating-cooling and ionization-neutralization reactions. At the end of the calculation, the code will identify the longest timescale for significant physical processes. A warning is produced if the user sets the age of the cloud and the code determines that the time-steady assumption is not valid. (The code can perform time-dependent calculations [Ferland & Truran 1981], although this has not been an emphasis in its development.)

6.3. The CLOUDY Test Suite

A large suite of test models has been developed to exercise the code fully over its intended range of validity. This serves to track changes in predictions over time. Many well-defined asymptotic limits are also tested, along with the standard nebular benchmark nebulae (Pequignot 1986; Ferland et al. 1995). Finally, codes to drive CLOUDY and to generate many large grids are included to exercise the code over its full range.

This suite of tests is computed on a regular basis, on a wide variety of platforms. We confirm that the code gets similar results on all platforms and monitor how these change with time.

6.4. Independent Verification—The Lexington Meeting

It is difficult to validate a numerical simulation fully, since analytical answers are seldom known. In the end, the only real way to verify that the calculation has been performed correctly is to compare results of fully independent calculations.

Daniel Pequignot organized a Workshop on Model Nebulae in 1985 (Pequignot 1986). This gave workers the opportunity to come together to compare predictions of various codes. The Lexington Meeting on Model Nebulae was held in 1994 with a similar goal, as well as part of the 70th birthday tribute to Don Osterbrock and Mike Seaton (Ferland et al. 1995). Such meetings provide a forum to discuss advances in atomic physics and numerical methods and to uncover bugs.

As a result of comparisons and discussions in the Lexington Meeting, the default continuum transfer method was changed from on-the-spot (OTS) to outward only (OO). Three types of transfer methods were represented by codes at the meeting. Two (those of Pat Harrington and Bob Rubin) used exact radiative transfer. The others used either OO or OTS. The OTS approximation ignores recombinations to the ground state since they are countered by an immediate ionization. In the OO approximation, recombinations to ground are counted, and the resulting radiation is added to an outward beam. The main difference between the two assumptions is in the temperature at the illuminated face of the cloud. This is because, for a gas heated mainly by photoionization of hydrogen, the heating rate is set by the local recombination rate. The recombination coefficient is only 2/3 as large in OTS as under OO, and the heating rates differ by this amount. Temperatures run hotter in

OO, as much as 10% hotter for conventional nebulae. OO did produce much better agreement with the exact codes.

As a result of this change, C90 tends to have higher temperatures at the illuminated face than those found by C84. This can increase the intensities of lines formed there, by 20%–30% but has little overall effect on the spectrum. The temperature at the illuminated face is quite sensitive to these details and so is likely to change when more exact radiative transfer methods are incorporated.

6.5. CLOUDY Version Numbers and Mailing List

The predicted spectrum is the result of a host of micro-physical processes, all with cross sections and rate coefficients that improve with time. Numerical methods are improved as workstations grow ever faster. Bugs are exposed and fixed. The result is that the code and its predictions change with time. These changes are documented on the CLOUDY Web site described below. The code uses version numbers to track these changes.

Integer increments to the version numbers are the result of significant changes to the structure or database within the code. The current version is 90. Minor changes, often bug fixes or changes to specific atomic cross sections or rates, are indicated by changes in the hundredths decimal place. At this writing the current version is 90.04. Very minor changes, often to fix specific problems, are indicated by letters following this. As an example, the last version of C84 was 84.12a.

A mailing list is maintained to notify interested parties of these changes, as they occur. Instructions for being placed on this mailing list are given on the CLOUDY Web site, described next.

7. WEB ACCESS

7.1. CLOUDY and Its Documentation

The CLOUDY Web site⁵ provides access to the FORTRAN source, the entire suite of test cases, the resulting output on various platforms, and the code's documentation, Hazy, A Brief Introduction to CLOUDY.

The source now consists of roughly 120,000 lines of FORTRAN. This is currently written in a mixture of FORTRAN 77 and a few FORTRAN 90 extensions (mainly the MilSpec do while and enddo statements). The code compiles, executes, and obtains similar answers on Sparcs, Dec Alphas, a Cray, Intel Windows NT, SGIs, and the HP Exemplar at the University of Kentucky Center for Computational Sciences. The resulting output from the entire test suite on these platforms is also posted. The intention here is to provide the ability to revalidate the code when it is run on platforms not included in our tests.

Hazy, the code's documentation, now consists of ~500 pages

⁵ <http://www.pa.uky.edu/~gary/cloudy>.

broken into four volumes (Ferland 1996).⁶ The first consists of a complete description of the input commands and their format. The second is a discussion of the physics and the numerical methods used. The third gives a discussion of machine-specific issues, the test cases, and information on how to use CLOUDY as a subprogram of other codes. Part 4 describes the output generated by the code and gives a list of the predicted emission lines. On the Web site, these are available in two formats, PostScript and Portable Document Format (PDF).

No matter how carefully the code is debugged and how many test cases are computed, it is inevitable that bugs will slip by undetected, only to be revealed later. This is simply a fact of life in anything as complex as CLOUDY. Other changes occur as the atomic database or numerical methods are expanded. The Web site contains the definitive list of changes to the code as it evolves through its versions. Within a static version, small changes to the code that fix specific late-appearing problems are listed as a set of hot fixes. These corrections must be made to the distributed source after it is downloaded and are not included in the distributed test output. This provides a facile method of making specific fixes to problems that are uncovered as the code is tested across the user community.

7.2. Independent Access to Atomic Data

Very large quantities of atomic and molecular data are needed for any spectroscopic simulation. This forms the foundation for a code like CLOUDY and is easily a full-time task. Since this work has application beyond CLOUDY itself, we have established the Atomic Data for Astrophysics (ADfA) Web site⁷ as a means of providing independent public access to this data.

7.2.1. Summary of ADfA

The basic atomic data compiled by ADfA and presented in convenient and compact form are readily used by developers of spectral synthesis codes needed for interpretation of new spectroscopic observations. New atomic data of astrophysical interest are being produced by many groups of atomic physicists, and the published data are spread among many journals. It is essential to have them evaluated and compiled in one place, keeping in mind the requirements of astrophysical quantitative spectroscopy.

The ADfA "philosophy" is to provide a complete set of the best available data and to upgrade them as soon as better data become publicly available. The ADfA provides on line all the basic ionization and recombination rates for the first 30 elements in convenient format. The present version of the ADfA is organized by category of data and includes the following sections:

Photoionization.

Recombination.

Collisional ionization and autoionization.

Charge transfer.

Auger processes.

Energy levels, wavelengths, and transition probabilities.

Collision strengths and excitation rates.

Stark broadening.

Opacities.

FORTTRAN subroutines.

The ADfA currently contains more than 8 Mbytes of information broken into 89 files, including 37 atomic data files (with more than 367,000 data entries), five FORTTRAN subroutines, and 47 supplementary files (data descriptions, PostScript, and LaTeX files of the corresponding papers). The ADfA also provides 66 external links to atomic data in electronic form stored at other locations accessible through the Internet. The ADfA home page has been visited more than 7000 times from 1995 October to 1997 December, and more than 12,000 files have been retrieved by users outside the University of Kentucky. The ADfA is a dynamic, regularly updated database.

8. DISCUSSION AND THE FUTURE

The section outlines the direction future work will take and describes what we view as the greatest uncertainties—the atomic data.

8.1. Atomic Data Needs

Oscillator and collisions strengths are needed for all emission lines. Fortunately the Opacity Project (Seaton 1987) and its extensions have produced a large body of high-quality line data. The majority of the most important emission lines now have high-quality data. Unfortunately this is not true for the physical processes that determine emission from hydrogen or helium and the ionization balance of the heavy elements. The following sections outline the greatest needs, from our experience.

8.1.1. Collisional Data for H and He

For hydrogen there are a variety of collision rates that are not in good agreement (Chang et al. 1991). The main need here is for accurate excitation and ionization rates for excited states. The situations for He⁰ and He⁺ are not much different; we know of no sources for collisions between highly excited levels or collisional ionization from them.

8.1.2. Dielectronic Recombination of Heavy Elements

A major error will be introduced if the recombination or ionization rates for the heavy elements are *systematically* under- or overestimated. It is easy to see why. Often thermodynamics sets the peak of the ionization distribution of a particular element at a given temperature. If the ionization or recombination rates are systematically too large or small by a relative error ε , then the ionization balance n stages from peak will have a cumulative error of $(1 - \varepsilon)^n$. This could be a very large error if ε and n are significant. The result is that the ionization

⁶ <http://www.pa.uky.edu/~gary/cloudy>.

⁷ <http://www.pa.uky.edu/~verner/atom.html>.

distribution may be quite uncertain far from the peak. In fact, over the history of CLOUDY, ionization fractions far from the peak have been the most variable.

The recombination database is now the greatest single uncertainty. The rates calculated by Nussbaumer & Storey for second-row elements and a few third-row ions remain the definitive ones because they used experimental energies for the autoionizing levels and had only to compute the transition probabilities. *Experimental energies for autoionizing levels are not known for most third- or fourth-row elements.*

In photoionization equilibrium, free electrons will have energies that are small compared to the ionization potential of the parent ion. Only those autoionizing levels very close to threshold participate in dielectronic recombination. At 10^4 K, only levels within 1 eV of threshold are significant, while the ionization energy is typically 30–50 eV. Ab initio theory would have to predict the positions of unobserved resonances with accuracy substantially better than 0.1 eV. Although it is possible to run large atomic structure codes to generate theoretical energy levels, there are no experimental measurements for comparison.

Within the theoretical uncertainty, a level predicted to be autoionizing might actually be bound. In this case the level can be populated only by three-body or radiative recombination, not dielectronic recombination. This fundamental uncertainty prevented Nussbaumer & Storey from computing rates for fourth-row or most third-row elements. The obvious solution is to perform the laboratory spectroscopy to determine experimentally the electronic structure.

The second concern is whether the population of the autoionizing levels is really in LTE. For instance, some low-lying autoionizing levels are not connected to the ground of the parent ion by an electric dipole transition, so slower processes will populate the level. NS83, NS84, NS86, and NS87 computed two sets of rates, one for the case in which the levels are not populated and a second for the case in which they are. This represents a systematic uncertainty in the recombination rates. Recent work by Savin et al. (1997) has shown the importance of levels that are not coupled to the recombined species by an *LS* coupling-allowed transition.

8.1.3. Charge Transfer

Charge transfer is a collision process that is treated on a molecular basis. The interaction potential for the approaching hydrogen atom–target ion system has an avoided crossing with the potential curve of the recombined ion–receding ion system.

The interaction is sensitive to the details of this avoided crossing, and the rates generally have significantly larger uncertainties than ionic collision rates. Kingdon & Ferland (1996) summarize the available data for atomic hydrogen impacting on the first four ions of the lightest 30 elements. In some cases new Landau-Zenner approximation rates were calculated. These may have an accuracy of ~ 1 dex. Even the best quantal rates have uncertainties approaching a factor of 2.

The effects of charge transfer on the resulting ionization distribution are highlighted by the recent study of the charge transfer between atoms and highly ionized species (Ferland et al. 1997). They found that order-of-magnitude changes in the ionization distribution of iron resulted from including estimates of the charge transfer rates of highly ionized species. Another extreme case is the Fe⁺ balance. The fits to photoionization cross sections presented by Verner et al. (1996a) and used here employ recent Iron Project data and differ from the Reilman & Manson cross sections by very large factors, approaching 10^3 in some cases. The resulting ionization balance of iron did not change when these data were incorporated in the first version of C90 (released in mid-1996) since charge transfer dominates the equilibrium balance. Nahar, Bautista, & Pradhan's (1997) claim that the ratio of Fe II to Fe I increases by a factor about 3–30 when the new photoionization data were incorporated was based on their neglect of charge transfer.

CLOUDY has been generously supported by the National Science Foundation, most recently by AST 96-17083. NASA has provided additional help through its LTSA program (NAGW 3315) and ATP grant GSFC-123. The University of Kentucky's Center for Computational Sciences, and its Director, John Connally, have generously supported Nebular Astrophysics at the University of Kentucky. Sumner Starrfield carefully reviewed the manuscript and made many suggestions. C90 was first released in June of 1996. During the succeeding time, the comments of Dana Balser, Mike Brotherton, Simon Casassus, Jane Charlton, Weihsueh Chiu, Mark Elowitz, Brian Espey, Mike Goad, Uffe Hellsten, John Houck, George Jacoby, John Kartje, Randolph Klein, Mike Kopko, Vincent Le Brun, Anthony Leonard, Valentina Luridiana, Bhaswati Mookerjee, Paul O'Brien, Tino Oliva, Enrique Perez, Rafael Reyes, Dimitra Rigopoulou, Ravi Sankrit, Sandra Savaglio, Greg Schwarz, Eric Shulman, Jon Slavin, Randall Smith, Stephanie Snedden, Henrik Spoon, Michele Thornley, Karen Vanlandingham, Peter van Hoof, Kevin Volk, James Wadsley, and Bob Williams helped in finding problems.

REFERENCES

- Aggarwal, K. M. 1983a, *J. Phys. B*, 16, L59
 ———. 1983b, *MNRAS*, 202, 15P
 ———. 1984, *ApJS*, 54, 1
 ———. 1985, *A&A*, 146, 149
 Aggarwal, K. M., Callaway, J., Kingston, A. E., & Unnikrishnan, K. 1992, *ApJS*, 80, 473
 Aldrovandi, S., & Pequignot, D. 1972, *A&A*, 17, 88
 ———. 1974, *Rev. Brasileira de Fis.*, 4, 491
 Ali, B., Blum, R. D., Bumgardner, T. E., Cranmer, S. R., Ferland, G. J., Haefner, R. I., & Tiede, G. P. 1991, *PASP*, 103, 1182
 Allard, N., Artru, M.-C., Lanz, T., & Le Dournef, M. 1990, *A&AS*, 84, 563

- Arnaud, M., & Raymond, J. 1992, *ApJ*, 398, 394
 Arnaud, M., & Rothenflug, R. 1985, *A&AS*, 60, 425
 Badnell, N. R. 1991, *ApJ*, 379, 356
 Baldwin, J. A., et al. 1996, *ApJ*, 461, 683
 Baldwin, J. A., Ferland, G. J., Korista, K. T., & Verner, D. 1995, *ApJ*, 455, L119
 Baluja, K. L. 1985, *J. Phys. B*, 18, L413
 Baluja, K. L., & Zeippen, C. J. 1988, *J. Phys. B* 21, 1455
 Bautista, M. A., & Pradhan, A. K. 1995, *J. Phys. B*, 28, L173
 Bely, O., & Van Regemorter, H. 1970, *ARA&A*, 8, 329
 Berrington, K. A. 1985, *J. Phys. B*, 18, L395
 ———. 1988, *J. Phys. B*, 21, 1083
 Berrington, K. A., Burke, P. G., Dufton, P. L., & Kingston, A. E. 1985, *At. Data Nucl. Data Tables*, 33, 195
 Bertoldi, F., & Draine, B. 1996, *ApJ*, 458, 222
 Bhatia, A. K., & Doscheck, G. A. 1995, *At. Data Nucl. Data Tables*, 60, 9
 Bhatia, A. K., & Mason, H. E. 1986, *A&A*, 155, 413
 Binette, L., Wang, J., Zuo, L., & Margris, C. 1993, *AJ*, 105, 797
 Blum, R. D., & Pradhan, A. K. 1992, *ApJS*, 80, 425
 Brage, T., Froese Fischer, C., & Judge, P. G. 1995, *ApJ*, 445, 457
 Brage, T., Hibbert, A., & Leckrone, D. S. 1997, *ApJ*, 478, 423
 Brage, T., Judge, P. G., & Brekke, P. 1996, *ApJ*, 464, 1030
 Brown, R. L., & Mathews, W. G. 1970, *ApJ*, 160, 939
 Burgess, A. 1965, *ApJ*, 141, 1588
 Burgess, A., & Percival, I. C. 1968, *Adv. Atom. Mol. Phys.*, 4, 109
 Burke, V. M., Lennon, D. J., & Seaton, M. J. 1989, *MNRAS*, 236, 353
 Butler, K., & Zeippen, C. J. 1984, *A&A*, 141, 274
 ———. 1994, *A&AS*, 108, 1
 Butler, S. E., & Dalgarno, A. 1980, *ApJ*, 241, 838
 Calamai, A. G., & Johnson, C. E. 1991, *Phys. Rev. A*, 44, 218
 Calamai, A. G., Smith, P. L., & Bergeson, S. D. 1993, *ApJ*, 415, L59
 Callaway, J. 1994, *At. Data Nucl. Data Tables*, 57, 9
 Callaway, J., Unnikrishnan, K., & Oza, D. H. 1987, *Phys. Rev. A*, 36, 2576
 Chandra, S. 1982, *Sol. Phys.*, 75, 133
 Chang, E. S., Avrett, E. H., & Loeser, R. 1991, *A&A*, 247, 580
 Chidichimo, M. C. 1981, *J. Phys. B*, 14, 4149
 Cochrane, D. M., & McWhirter, R. W. P. 1983, *Phys. Scr.*, 28, 25
 Cota, S. A. 1987, Ph.D. thesis, Ohio State Univ.
 Davidson, K. 1972, *ApJ*, 171, 213
 ———. 1975, *ApJ*, 195, 285
 Davidson, K., & Netzer, H. 1979, *Rep. Prog. Phys.*, 51, 715
 Dopita, M. A., Mason, D. J., & Robb, W. D. 1976, *ApJ*, 207, 102
 Dufton, P. L., Brown, P. J. F., Lennon, D. J., & Lynas-Gray, A. E. 1986a, *MNRAS*, 222, 713
 Dufton, P. L., Doyle, J. G., & Kingston, A. E. 1979, *A&A*, 78, 318
 Dufton, P. L., Hibbert, A., Keenan, F. P., Kingston, A. E., & Doschek, G. A. 1986b, *ApJ*, 300, 448
 Dufton, P. L., Hibbert, A., Kingston, A. E., & Doschek, G. A. 1982, *ApJ*, 257, 338
 Dufton, P. L., & Kingston, A. E. 1984, *J. Phys. B*, 17, 3321
 ———. 1987, *J. Phys. B*, 20, 3899
 ———. 1989, *MNRAS*, 241, 209
 ———. 1991, *MNRAS*, 248, 827
 ———. 1994, *At. Data Nucl. Data Tables*, 57, 273
 Dumont, A. M., & Mathez, G. 1981, *A&A*, 102, 1
 Elitzur, M., & Ferland, G. J. 1986, *ApJ*, 305, 35
 Fang, Z., & Kwong, H. S. 1997, *ApJ*, 483, 527
 Federman, S. R., & Shipsey, E. J. 1983, *ApJ*, 269, 791
 Ferguson, J., & Ferland, G. J. 1997, *ApJ*, 479, 363 (FF)
 Ferland, G. J. 1992, *ApJ*, 389, L63
 Ferland, G. J. 1996, Hazy, a Brief Introduction to CLOUDY 90, Univ. of Kentucky Physics Department Internal Report
 Ferland, G. J., Baldwin, J. A., Korista, K. T., Hamann, F., Carswell, R., Phillips, M., Wilkes, B., & Williams, R. E. 1996, *ApJ*, 461, 683
 Ferland, G., et al. 1995, in *The Analysis of Emission Lines*, ed. R. Williams & M. Livio (Cambridge: Cambridge Univ. Press), 83
 Ferland, G. J., Fabian, A. C., & Johnstone, R. M. 1994, *MNRAS*, 266, 399
 Ferland, G. J., Korista, K. T., Verner, D. A., & Dalgarno, A. 1997, *ApJ*, 481, L115
 Ferland, G. J., & Persson, S. E. 1989, *ApJ*, 347, 656
 Ferland, G. J., & Rees, M. J. 1988, *ApJ*, 332, 141
 Ferland, G. J., & Truran, J. W. 1981, *ApJ*, 244, 1022
 Fleming, J., Bell, K. L., Hibbert, A., Vaeck, N., & Godefroid, M. R. 1996, *MNRAS*, 279, 1289
 Fleming, J., Brage, T., Bell, K. L., Vaeck, N., Hibbert, A., Godefroid, M. R., & Froese Fischer, C. 1995, *ApJ*, 455, 758
 Flower, D. R. 1976, *A&A*, 56, 451
 Froese Fischer, C. 1983, *J. Phys. B*, 16, 157
 ———. 1995, *ApJ*, 455, 758
 Gaetz, T. J., & Salpeter, E. E. 1983, *ApJS*, 52, 155
 Galavis, M. E., Mendoza, C., & Zeippen, C. J. 1995, *A&AS*, 111, 347
 Garstang, R. H. 1957, *Vistas Astron.*, 1, 268
 Garstang, R. H., Robb, W. D., & Rountree, S. P. 1978, *ApJ*, 222, 384
 Giles, K. 1981, *MNRAS*, 195, 63
 Grevesse, N., & Anders, E. 1989, in *AIP Conf. Proc.* 183, *Cosmic Abundances of Matter*, ed. C. J. Waddington (New York: AIP), 1
 Grevesse, N., & Noels, A. 1993, in *Origin and Evolution of the Elements*, ed. N. Prantzos, E. Vangioni-Flam, & M. Casse (Cambridge: Cambridge Univ. Press), 15
 Gruenwald, R., Viegas, S. M., & Broguiere, D. 1997, *ApJ*, 480, 283
 Hamann, F., & Ferland, G. J. 1993, *ApJ*, 418, 11
 Harrington, J. P. 1969, *ApJ*, 156, 903
 Hata, J., Morgan, L. A., & McDowell, M. R. C. 1980, *J. Phys. B*, 13, 4453
 Hayes, M. A. 1986, *J. Phys. B*, 19, 1853
 Hibbert, A., Godefroid, M. R., & Froese Fischer, C. 1995, *ApJ*, 455, 758
 Hjellming, R. M. 1966, *ApJ*, 143, 420
 Ho, Y. K., & Henry, R. J. W. 1984, *ApJ*, 282, 816
 Hollenbach, D., & McKee, C. F. 1989, *ApJ*, 342, 306
 Hummer, D. G. 1988, *ApJ*, 327, 477
 Hummer, D. G., Berrington, K. A., Eissner, W., Pradhan, A. K., Saraph, H. E., & Tully, J. A. 1993, *A&A*, 279, 298
 Hummer, D. E., & Storey, P. J. 1987, *MNRAS*, 224, 801
 Johansson, S., Brage, T., Leckrone, D. S., Nave, G., & Wahlgren, G. M. 1995, *ApJ*, 446, 361
 Johnson, C. T., Burke, P. G., & Kingston, A. E. 1987, *J. Phys. B*, 20, 2553
 Johnson, C. T., Kingston, A. E., & Dufton, P. L. 1986, *MNRAS*, 220, 155
 Kaastra, J. S., & Mewe, R. 1993, *A&AS*, 97, 443
 Kafatos, M., & Lynch, J. P. 1980, *ApJS*, 42, 611
 Kallman, T. R., & McCray, R. 1982, *ApJS*, 50, 263
 Kaufman, V., & Sugar, J. 1986, *J. Phys. Chem. Ref. Data*, 15, 321
 Keenan, F. P., Harra, L. K., Aggarwal, K. M., & Feibelman, W. A. 1992, *ApJ*, 385, 375
 Keenan, F. P., & Norrington, P. H. 1987, *A&A*, 181, 370
 Kingdon, J. B., & Ferland, G. J. 1996, *ApJS*, 106, 205
 Kingston, A. E. 1986, *Phys. Scr.* 34, 216
 Krueger, T. K., & Czyzak, S. J. 1970, *Proc. R. Soc. London A*, 318, 531

- Kwong, V., Fang, Z., Gibbons, T. T., Parkinson, W. H., & Smith, P. L. 1993, *ApJ*, 411, 431
- Leep, D., & Gallagher, A. 1976, *Phys. Rev. A*, 13, 148
- Lennon, D. J., & Burke, V. M. 1991, *MNRAS*, 251, 628
- . 1994, *A&AS*, 103, 273
- Lennon, D. J., Dufton, P. L., Hibbert, A., & Kingston, A. E. 1985, *ApJ*, 294, 200
- Lepp, S., & Shull, J. M. 1983, *ApJ*, 270, 578
- MacAlpine, G. M. 1971, *ApJ*, 175, 11
- Mason, H. 1975, *MNRAS*, 170, 651
- Mathews, W. G., & Ferland, G. J. 1987, *ApJ*, 323, 456
- McGuire, E. 1993, *Writing Solid Code* (Redmond, WA: Microsoft)
- McLaughlin, B. M., & Bell, K. L. 1993, *ApJ*, 408, 753
- Mendoza, C. 1982, in *IAU Symp. 103, Planetary Nebulae*, ed. D. R. Flower (Dordrecht: Reidel), 143
- Mendoza, C., & Zeppen, C. J. 1982a, *MNRAS*, 198, 127
- . 1982b, *MNRAS*, 199, 1025
- . 1983, *MNRAS*, 202, 981
- . 1987, *MNRAS*, 224, 7P
- Mewe, R. 1972, *A&A*, 20, 215
- Mohan, M., Hibbert, A., & Kingston, A. E. 1994, *ApJ*, 434, 389
- Muhlethaler, H. P., & Nussbaumer, H. 1976, *A&A*, 48, 109
- Nahar, S. N., Bautista, M. A., & Pradhan, A. K. 1997, *ApJ*, 479, 497
- Nahar, S. N., & Pradhan, A. K. 1994, *J. Phys. B*, 27, 429
- Netzer, H. 1990, in *Active Galactic Nuclei, Saas-Fee Advanced Course 20*, ed. T. J.-L. Courvoisier & M. Mayor (Berlin: Springer), 57
- Neufeld, D. A., & Dalgarno, A. 1987, *Phys. Rev. A*, 35, 3142
- Nussbaumer, H. 1986, *A&A*, 155, 205
- Nussbaumer, H., & Rusca, C. 1979, *A&A*, 72, 129
- Nussbaumer, H., & Storey, P. J. 1981, *A&A*, 99, 177
- . 1982, *A&A*, 113, 21
- . 1983, *A&A*, 126, 75 (NS83)
- . 1984, *A&AS*, 56, 293 (NS84)
- . 1986, *A&AS*, 64, 545 (NS 86)
- . 1987, *A&AS*, 69, 123 (NS87)
- . 1988, *A&A*, 200, L25
- Oliva, E., Pasquali, A., & Reconditi, M. 1996, *A&A*, 305, 210
- Osterbrock, D. E. 1989, *Astrophysics of Gaseous Nebulae and Active Galactic Nuclei* (Mill Valley: University Science)
- Pelan, J., & Berrington, K. A. 1995, *A&AS*, 110, 209
- Pequignot, D. 1986, in *Workshop on Model Nebulae*, ed. D. Pequignot (Paris: l'Observatoire de Paris), 363
- Percival, I. C., & Richards, D. 1978, *MNRAS*, 183, 329
- Petitjean, P., Boisson, C., & Pequignot, D. 1990, *A&A*, 240, 242
- Ramsbottom, C. A., & Bell, K. L. 1997, *At. Data Nucl. Data Tables*, 66, 65
- Ramsbottom, C. A., Bell, K. L., & Keenan, F. P. 1997, *MNRAS*, 284, 754
- Ramsbottom, C. A., Bell, K. L., & Stafford, R. P. 1996, *At. Data Nucl. Data Tables*, 63, 57
- Ramsbottom, C. A., Berrington, K. A., & Bell, K. L. 1995, *At. Data Nucl. Data Tables*, 61, 105
- Ramsbottom, C. A., Berrington, K. A., Hibbert, A., & Bell, K. L. 1994, *Phys. Scr.*, 50, 246
- Rees, M. J., Netzer, H., & Ferland, G. J. 1989, *ApJ*, 347, 640
- Reilman, R. F., & Manson, S. T. 1979, *ApJS*, 40, 815, errata 1981, 46, 115; 1986, 62, 939
- Rubin, R. H. 1968, *ApJ*, 153, 671
- Rybicki, G. B., & Lightman, A. P. 1979, *Radiative Processes in Astrophysics* (New York: Wiley-Interscience)
- Saha, H. P., & Treffitz, E. 1982, *A&A*, 116, 224
- . 1983, *Sol. Phys.*, 87, 233
- Sampson, D. H., & Zhang, H. L. 1988, *ApJ*, 335, 516
- Samson, J. A. R., He, Z. X., Yin, L., & Haddad, G. N. 1994, *J. Phys. B*, 27, 887
- Saraph, H. E. 1970, *J. Phys. B*, 3, 952
- Saraph, H. E., & Storey, P. J. 1996, *A&AS*, 115, 151
- Saraph, H. E., Storey, P. J., & Tully, J. A. 1995, in *5th Internat. Colloq. on Atomic Spectra and Oscillator Strengths*, ed. W.-U. L. Tchang-Brillet, J.-F. Wyart, & C.J. Zeippen (Meudon: Publications de l'Observatoire de Paris), 110
- Saraph, H. E., & Tully, J. A. 1994, *A&AS*, 107, 29
- Savin, D. W., et al. 1997, *ApJ*, 489, L118
- Sawey, P. M. J., & Berrington, K. A. 1993, *At. Data Nucl. Data Tables*, 55, 81
- Seaton, M. J. 1959, *MNRAS*, 119, 90
- . 1962, in *Atomic and Molecular Processes*, ed. D. Bates (New York: Academic), 375
- . 1964, *Planet. Space Sci.*, 12, 55
- . 1987, *J. Phys. B*, 20, 6363
- Shields, G. A. 1974, *ApJ*, 191, 309
- Shull, J. M., & Van Steenberg, M. E. 1982, *ApJS*, 48, 95
- . 1985, *ApJ*, 298, 268
- Sigut, A., & Pradhan, A. K. 1995, *J. Phys. B*, 28, 4879
- Stafford, R. P., Bell, K. L., Hibbert, A., & Wijesundera, W. P. 1994, *MNRAS*, 268, 816
- Stafford, R. P., Hibbert, A., & Bell, K. L. 1993, *MNRAS*, 260, L11
- Stasinska, G., & Leitherer, C. 1996, *ApJS*, 107, 661
- Stepney, S., & Guilbert, P. W. 1983, *MNRAS*, 204, 1269
- Storey, P. J., & Hummer, D. G. 1995, *MNRAS*, 272, 41
- Storey, P. J., Mason, H. E., & Saraph, H. E. 1996, *A&A*, 309, 677
- Sugar, J., & Corliss, C. 1985, *Atomic Energy Levels of the Iron-Period Elements, Potassium through Nickel* (*J. Phys. Chem. Ref. Data*, 14) (New York: NBS)
- Summers, H. P. 1974, *Appleton Laboratory Report AL-R-5*
- Sutherland, R., & Dopita, M. 1993, *ApJS*, 88, 253
- Swings, P., & Struve, O. 1940, *ApJ*, 91, 546
- Tayal, S. S. 1997, *ApJ*, 481, 550
- Tayal, S. S., Burke, P. G., & Kingston, A. E. 1985, *J. Phys. B*, 18, 4321
- Tayal, S. S., & Henry, R. J. W. 1986, *ApJ*, 302, 200
- Tayal, S. S., Henry, R. J. W., & Pradhan, A. K. 1987, *ApJ*, 319, 951
- Tielens, A. G. G., & Hollenbach, D. 1985, *ApJ*, 291, 722
- van Regemorter, H. 1962, *ApJ*, 136, 906
- Verner, D. A., & Ferland, G. J. 1996, *ApJS*, 103, 467
- Verner, D. A., Ferland, G. J., Korista, K. T., & Yakovlev, D. G. 1996a, *ApJ*, 465, 487
- Verner, D. A., Verner, E. M., & Ferland, G. J. 1996b, *At. Data Nucl. Data Tables*, 64, 1
- Verner, D. A., & Yakovlev, D. G. 1990, *ApSS*, 165, 27
- . 1995, *A&AS*, 109, 125
- Voronov, G. S. 1997, *At. Data Nucl. Data Tables*, 65, 1
- Vriens, L., & Smeets, A. H. M. 1980, *Phys. Rev. A*, 22, 940
- Wahlgren, G. M. 1995, *ApJ*, 446, 361
- Weisheit, J. C. 1974, *ApJ*, 190, 735
- Weisheit, J. C., & Collins, L. A. 1976, *ApJ*, 210, 299
- Weisheit, J. C., & Dalgarno, A. 1972, *Astrophys. Lett.*, 12, 103
- Wiese, W. L., Fuhr, J. R., & Deters, T.M. 1996, *Atomic Transition Probabilities of Carbon, Nitrogen, and Oxygen: A Critical Data Compilation* (*J. Phys. Chem. Ref. Data, Monograph 7*) (Washington, DC: National Institute of Standards and Technology)
- Wiese, W. L., Smith, M. W., & Glennon, B. M. 1966, *Atomic Transition Probabilities: A Critical Data Compilation* (NSRDS-NBS, 4) (Washington, DC: NBS)
- Williams, R. E. 1967, *ApJ*, 147, 556
- Wills, B. J., Wills, D., & Netzer, H. 1985, *ApJ*, 288, 143
- Wills, D., & Netzer, H. 1979, *ApJ*, 233, 1

Xu, Y., & McCray, R. 1991, *ApJ*, 375, 190

Zeppen, C. J. 1982, *MNRAS*, 198, 111

———. 1990, *A&A*, 229, 248

Zeppen, C. J., Le Bourlot, J., & Butler, K. 1987, *A&A*, 188, 251

Zhang, H. L., Graziani, M., & Pradhan, A. K. 1994, *A&A*, 283, 319

Zygelman, B., & Dalgarno, A. 1987, *Phys. Rev. A*, 35, 4085

———. 1990, *ApJ*, 365, 239